

Electrochemical Migration of Micro-alloyed Low Ag Solders in NaCl Solution

Bálint Medgyes / Balázs Illés / Gábor Harsányi

RESEARCH ARTICLE

Received 2013-03-21, revised 2013-05-07, accepted 2013-05-13

Abstract

The reliability investigation of lead-free solders is still a current issue. In this paper, Electrochemical Migration (ECM) behaviour of novel lead-free micro-alloyed low Ag content solders was investigated by water drop test in NaCl solution. The results were compared to commonly used lead-free and lead bearing solder alloys. It was found that some micro-alloyed solders can have as low ECM susceptibility as lead bearing ones. X-ray photoelectron spectroscopy was also carried out to find the root cause of different ECM behaviour of micro-alloyed solders. The results of water drop test and X-ray photoelectron spectroscopy were in good agreement in terms of electrochemical migration susceptibility, since SAC0807 solder alloy has shown higher corrosion rate than SAC0307 and has a higher ability for ECM as well. It is concluded that some lead-free micro-alloyed low Ag content solder alloys (e.g.: SAC0807) may pose a high reliability risk in electronic devices during operation.

Keywords

Electrochemical Migration · Micro-alloyed Solder · Water Drop test · XPS · Pitting Corrosion

Acknowledgement

The work reported in the paper has been developed in the framework of the "Talent care and cultivation in the scientific workshops of BME" project. This project is supported by the grant TÁMOP-4.2.2.B-10/1–2010-0009. The authors would also like to thank to Prof. Miklós Menyhárd and Sándor Gurbán for their efforts taken in connection with the XPS measurements.

Bálint Medgyes

Department of Electronics Technology, Faculty of Electrical Engineering and Informatics, Budapest University of Technology and Economics, Egrý József u. 18., H-1111 Budapest, Hungary
e-mail: medgyes@ett.bme.hu

Balázs Illés

Gábor Harsányi

Department of Electronics Technology, Faculty of Electrical Engineering and Informatics, Budapest University of Technology and Economics, Egrý József u. 18., H-1111 Budapest, Hungary

1 Introduction

In microelectronics industry, the applied solder materials are one of the most important factors related to the reliability of the products. According to the Restrictions of Hazardous Substances (RoHS) directive of European Union, lead bearing solders had to be replaced with lead-free ones [1]. In this context, alternative binary alloys had been examined as replacements for SnPb solders, such as near-eutectic SnAg, SnCu and SnZn alloys. However, ternaries (SnAgCu, SnZnAg, SnZnIn, etc.) and even quaternary alloys (SnZnAgAl, SnAgBiCu, SnInAgSb) had also been studied as candidates for lead-free solders [2–7].

The reliability investigation of lead-free solders is still a current issue. One of the important reliability topics is the electrochemical migration (ECM) failure phenomenon. The common characteristics of the ECM phenomenon include the presence of moisture on conductor-dielectric-conductor systems under bias voltage, the electrochemical process and the metallic dendrite growth. This process is driven by the applied electric field from the anode to the cathode. Dendrite growth occurs as a result of metal ions being dissolved into a solution from the anode and deposited at the cathode, thereby growing in needle or tree-like formations. This effect causes short-circuits in electronic circuits, which may lead to a catastrophic failure.

Many papers can be found about ECM investigations carried out on different lead-free solder alloys. Takemoto et al. have found that some tin based lead-free solder alloys are more resistant to ECM than Sn-Pb40 alloy and pure Indium. In-48Sn and In-50Pb alloys were found to be immune to ECM in high purity water [8]. Yu et al. have described that in Sn-37Pb and Sn-36Pb2Ag systems the main migration element is Pb, while in Sn-Ag and Sn-Ag-Cu solder alloys Sn leads the migration in high purity water [9, 10].

Other publication reported that SAC305 lead-free solder alloy has longer ECM lifetime in 0.001% NaCl solution than in 0.001% Na₂SO₄, since the passivity layer formed of SnO₂ is thicker in the case of NaCl solution and Sn is the only element that contributes to ECM at room temperature [11]. The migration behaviour and the deposition process of Sn, Cu and Ag in case of SAC305 solder alloy were also observed in a thermal-

humidity bias test (65°C/88%RH) [12].

Many studies were carried out on lead-free micro-alloyed low Ag content solders covering different reliability issues, like solderability, intermetallic compound (IMC) evaluation, shear strength behaviour [13], tensile and wettability properties [14] or electromigration behaviour [15] which is a phenomenon different from ECM. However, ECM investigations of the novel lead-free micro-alloyed low Ag content solders were not found in the literature.

ECM susceptibility is usually examined by environmental tests such as Thermal Humidity Test (THB) and Highly Accelerated Stress Test (HAST) or under normal conditions by Water Drop test (WD), Thin Electrolyte Layer (TEL) test and by polarization tests such as linear voltammetry [16–18]. ECM behaviour of metallisation or insulation material systems is usually determined by the Mean-Time-To-Failure (MTTF) values during THB, HAST and WD tests. During environmental tests, the water condensation time can have a high influence on the overall process and has a high impact on the calculated MTTF values [16], since ion migration starts only if a continuous condensed moisture film is present between the conductor traces. During WD tests there is no water condensation; the water droplet is placed on the surface and thereafter the migration process can start immediately.

In this paper, the electrochemical migration behaviour of lead-free micro-alloyed low Ag content solders was investigated by WD tests in NaCl solution. The results were compared with the ECM behaviour of commonly used SnAgCu and SnPb solder alloys. Moreover, X-ray Photoelectron Spectroscopy (XPS) measurements were also carried out to investigate the relation between the formed oxide layers and the ECM susceptibility of the solders.

2 Experimental

In order to carry out the WD tests, a standard comb pattern was designed according to the IPC-B-24 test board with the following main parameters: the raster of the conductor stripes was 0.4 mm with a gap size of 0.5 mm on an FR-4 substrate. The interdigital patterns were made by conventional photolithography and wet etching processes. The Cu base conductor was coated by immersion Sn for further reflow soldering processes. During this study the following solder alloys were investigated: Sn98.9Ag0.3Cu0.7Bi0.1Sb0.01 (SAC0307), Sn98.4Ag0.8Cu0.7Bi0.1 (SAC0807), Sn96.5Ag3Cu0.5 (SAC305), Sn95.5Ag4Cu0.5 (SAC405), Sn63Pb37 and Sn62Pb36Ag2 on standard comb pattern. The solder pastes were printed by a 150 µm stainless steel stencil and were reflowed according to a lead-free [190°C, 210°C(90 s), peak: 240°C(30 s)] and a lead bearing [150°C, 170°C(90 s), peak: 210°C(30 s)] soldering profile. In order to avoid the effect of fluxes [19], the same flux type was applied in all cases.

The applied test platform of WD tests can be seen in Fig. 1. During the WD tests a droplet of 15 µl 1 mM NaCl was placed by

a pipette onto the comb patterns and then 10 VDC was applied. The NaCl solution simulates the condensed sea water or other salty contaminants (e.g. human perspiration).

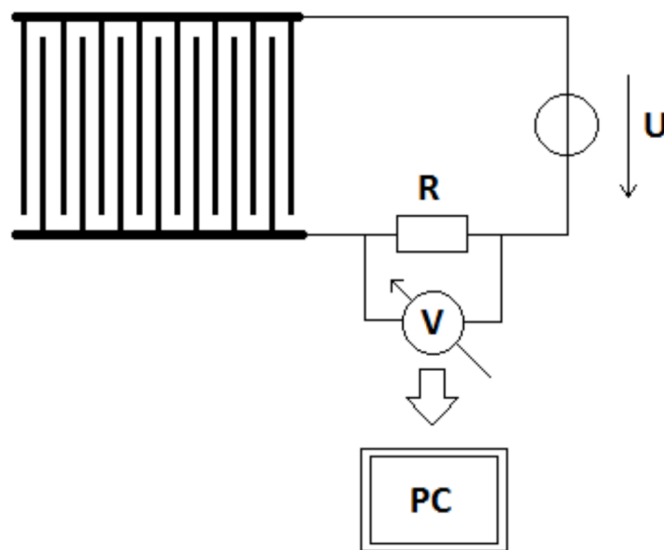


Fig. 1. Schematic of the real-time measuring platform for WD tests.

The short circuit formation (the time to failure) was detected by voltage step measurements on a resistor ($R = 1 \text{ k}\Omega$) connected in series to the interdigital structure. The applied failure criterion was 0.1 VDC (first dendrite appearance). The formation of dendrites was monitored visually as well by an optical microscope and 32 samples were tested from each type of solder.

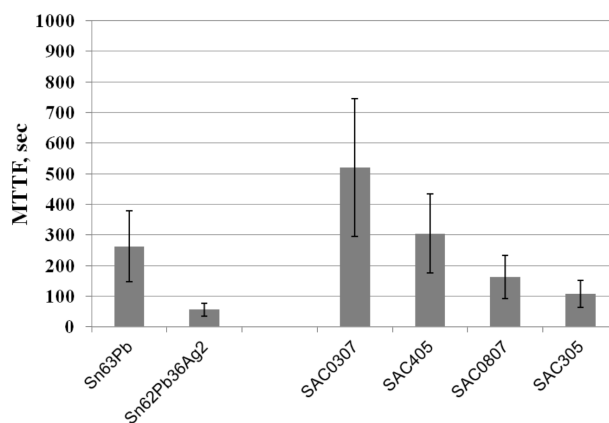


Fig. 2. MTTF of different solder alloys in 1mM NaCl solution.

From the measured failure times the Mean Time To Failure (MTTF) was calculated as an average value. The formed dendrites were also investigated by Scanning Electron Microscopy (SEM) in order to study their microstructures and by Energy Dispersive Spectroscopy (EDS) to analyse the elemental compositions. It has been assumed that oxide thickness (as a corrosion product) can have a strong influence on ECM susceptibility, in particular on the anodic dissolution rate. The formed oxide layers (anode side) were investigated by XPS depth profiling in order to make a relative comparison between the oxide

layer thicknesses on the solder surfaces after various treatments. The conditions for depth profiling were: optimized pressure, the samples were rotated during the sputtering to get 78° incidence angle of the beam. The Ar⁺ ions were accelerated by 1kV.

3 Results and Discussion

The WD test results of the different solder alloys can be observed in Fig. 2. The observed deviations were relatively high, since the ECM processes are not stationary and also the electrochemical cell platforms are not homogeneous. Therefore there are no available exact relationships, only empirical models [16, 20, 21]. Despite the huge deviations, an ECM ranking could be established. According to the expectations, the reference Pb-bearing solder alloys showed a relatively high ECM susceptibility compared to the lead-free ones [10]. Interestingly, SAC305 and SAC0807 solder alloys showed similarly low ECM resistance and even worse ECM resistance values compared to Sn63Pb37. The following ECM susceptibility ranking can be established:

$$\text{SAC 305} \geq \text{SAC 0807} \geq \text{SAC 405} \geq \text{SAC 0307}$$

Tab. 1. EDS results of SAC0807 and SAC0307 dendrites.

Element	Norm. wt. [%]	Norm. at. [%]
SAC0807		
Tin	43.68	7.59
Carbon	46.87	80.49
Oxygen	8.94	11.53
Sodium	0.31	0.28
Chlorine	0.17	0.09
SAC0307		
Tin	51.52	10.4
Carbon	34.16	68.16
Oxygen	13.87	21.08
Sodium	0.25	0.22
Chlorine	0.2	0.12

It should be also noted that there is a significant MTTF difference between the low Ag content solder alloys (SAC0307 vs. SAC0807) in spite of their very similar compositions. Comparisons of microstructure and elemental composition were carried out in order to find the reason for this huge MTTF difference.

The typical microstructure of SAC0807 and SAC0307 can be seen in Figures 3 and 4. The dendrite grown from SAC0807 (Fig. 3) is coated by residues and the microstructure forms perpendicular angles. The dendrites originated from SAC0307 solder alloy show needle-like structures (Fig. 4).

According to the EDS analysis, Sn was detected as the main element of the dendrites in both sample types (see Table 1). Carbon and oxygen have mainly originated from the FR4 substrate,

Tab. 2. Sn_{oxide}/Sn_{all} ratios depending on the (un)treatment and depth.

T:treated U:untreated	oxide ratio (~ 50%)	oxide ratio (~ 15%)
03Cl:U	2–3 nm	12 nm
03Cl:T	20 nm	60 nm
08Cl:U	~0 nm	30 nm
08Cl:T	50 nm	> 200 nm

but oxygen could also come from the surface oxidation of the dendrites. Despite the high microstructural and MTTF differences between the SAC0807 and SAC0307 alloys, significant elemental composition differences were not detected in the dendrites.

The SEM and EDS results did not provide an adequate explanation of the significant MTTF differences between SAC0307 and SAC0807. Therefore XPS investigations were carried out to measure the formed oxide components on the anode surface: on an untreated area as a reference and on a treated area after WD test. According to our assumption, the formed oxide layer may have been caused by a kind of corrosion effect which can influence the ECM process.

The concentrations and/or ratios of pure and oxidized Sn components were calculated by the decomposition of the measured XPS spectra applying the 3d5/2 line of the pure Sn peak (see Fig. 5). The raw data of the Sn spectra was simply corrected for the background of the secondary photoelectron using the Shirley method [22]. The asymmetric XPS line shape of 3d5/2 peak is well represented by the combinations of Gaussian and Lorentzian functions.

An example of the deconvolution procedure is shown in Fig. 6.

The concentration of Sn in oxide binding (SnO_x) is shown by the deconvolution. The change of the valence state – the change of x along the depth – can be interpreted from the shift of the energy of the Sn XPS peak. Fig. 7. shows the oxidized Sn profile. It can be observed that on the surface probably a thin native oxide layer can be found. The amount of oxidized Sn falls below 50% under the depth of 2 nm and it is less than 15% under the depth of 14 nm.

The summary of the XPS results can be seen in Table 2. In every case a relative thick oxide layer has grown during the WD tests (after treatment). However, this oxide layer was not well defined in every case. A highly inhomogeneous oxide front has formed towards the vertical and the horizontal axis. An example of the vertically inhomogeneous appearance of oxide can be seen in Fig. 8. It can be supposed that this vertically and horizontally inhomogeneous oxide front was caused by the so called pitting corrosion.

Pitting corrosion is most commonly induced by chloride ions or other halides. These halides are very highly potent agents for destroying otherwise protective passive surface films such as an SnO₂ layer [23]. A possible formation mechanism of SnO₂ is

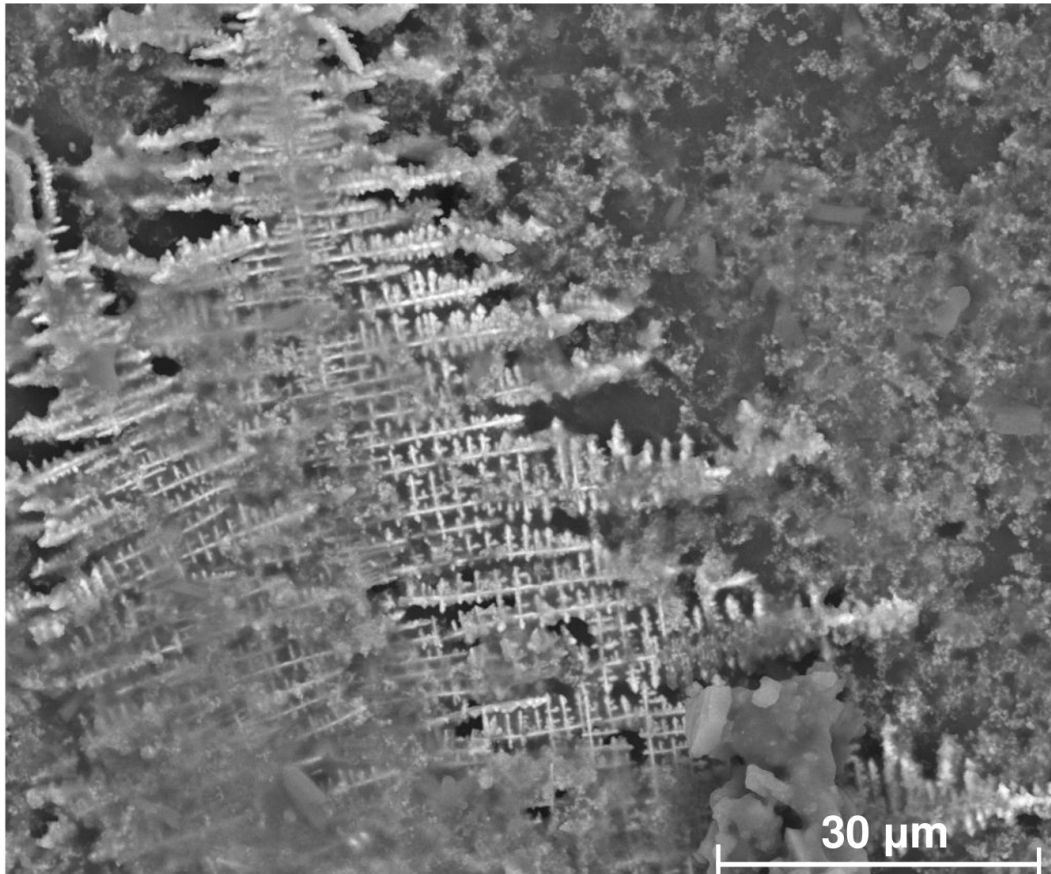


Fig. 3. SEM image of a dendrite; coated by residues, grown from SAC0807 during WD test.

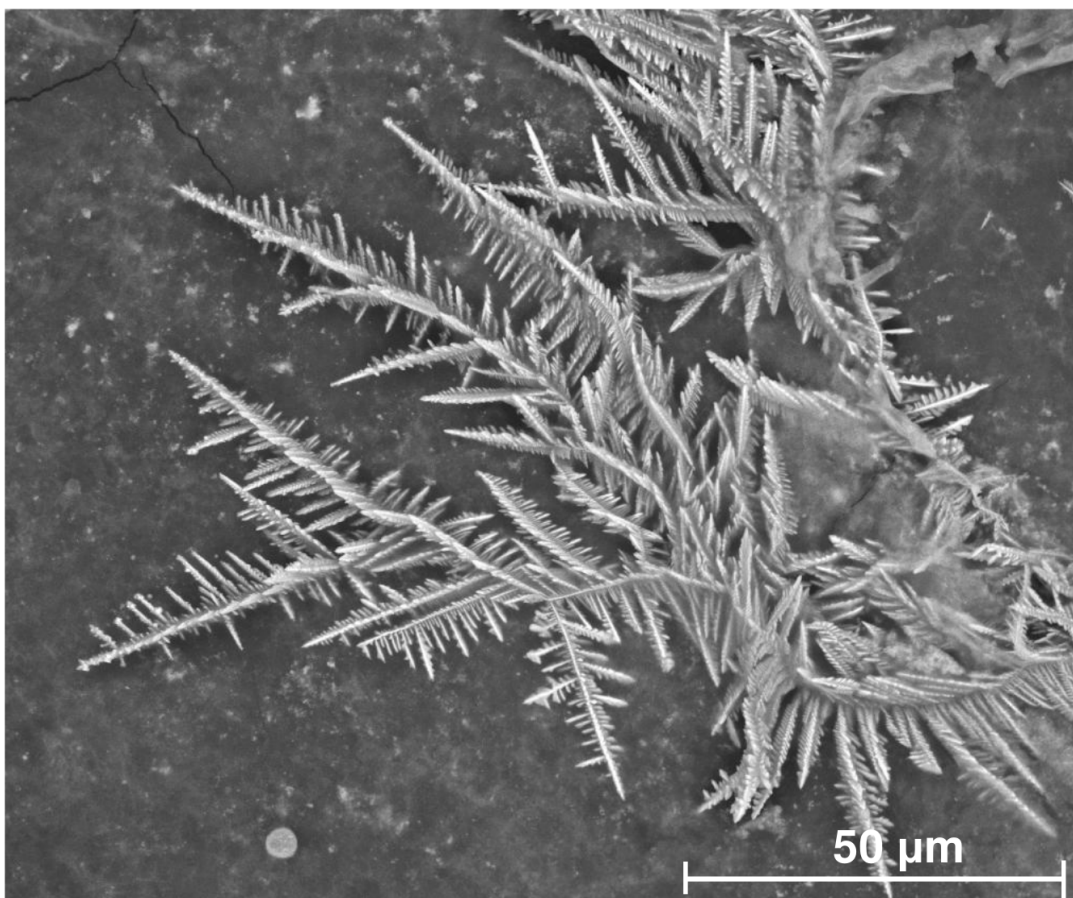


Fig. 4. SEM image of a dendrite; grown from SAC0307 during WD test.

Fig. 5. The 3d3/2 (left) and 3d5/2 (right) peaks of pure Sn.

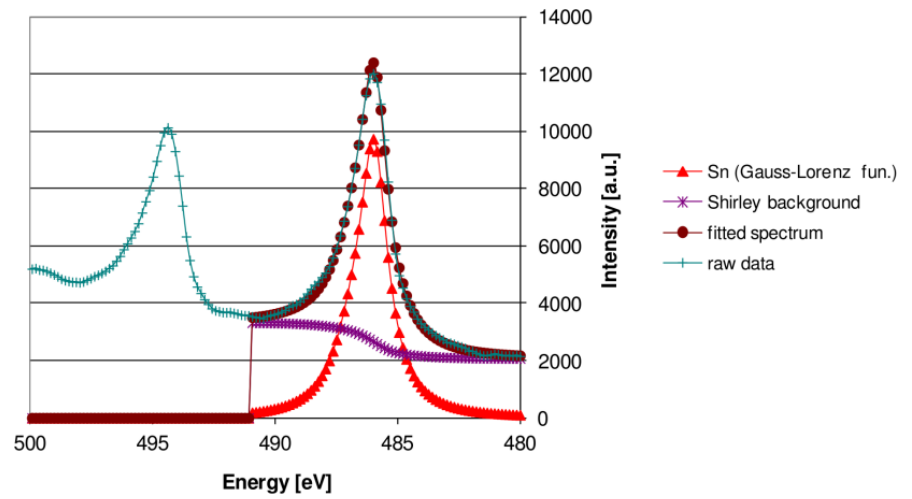


Fig. 6. Deconvolution of XPS spectrum of SAC0807 solder alloy; untreated sample; thickness of the removed material was 8nm.

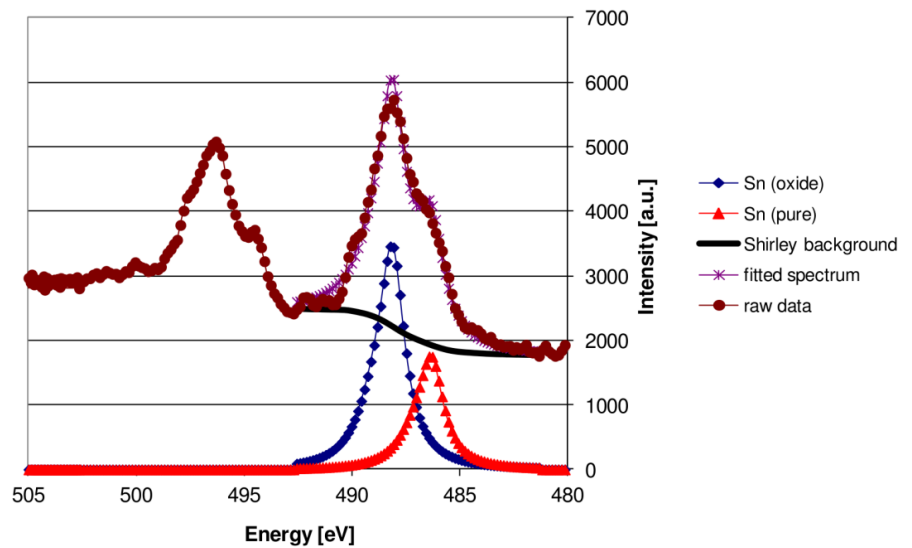
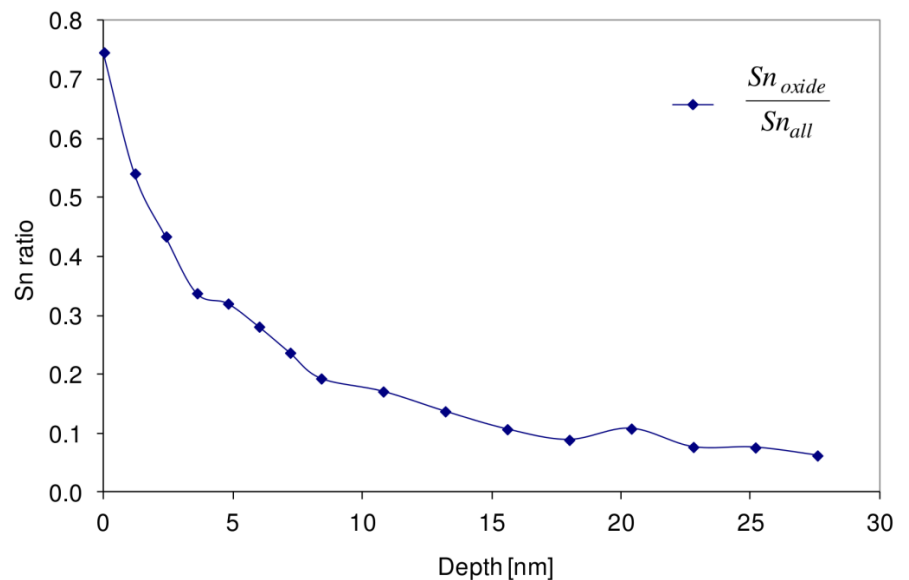
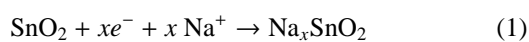


Fig. 7. XPS depth profile of SAC0307 solder alloy before WD test (untreated).



described by [24]:

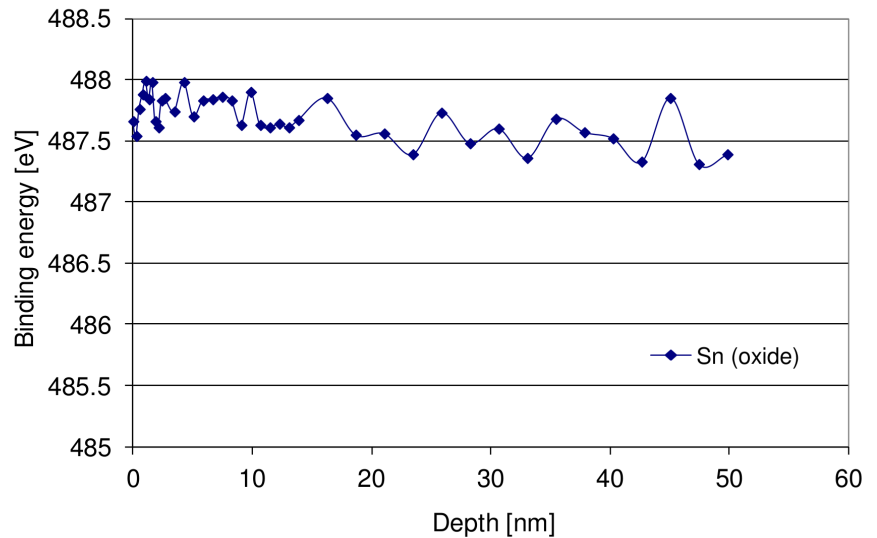


where $x = 1$ or 2 .

As mentioned above, an inhomogeneous oxidation front was formed, so the SnO_x passive layer was destroyed at different points of the area. It is called pitting corrosion.

The pitting corrosion mechanism also involves a strong chloride ion concentrating effect in the growing pits due to the applied positive charge potential at the anode. The chloride ions were facilitated to locally penetrate the material, especially at the imperfections of the SnO_x film. As it can be seen in Table 2, in case of the SAC0807 deeper pitting corrossions have developed than in case of the SAC0307 solder alloy. Accord-

Fig. 8. The change of the binding energy of oxidized tin atoms (O8Cl: untreated) as a function of the depth.



ingly, the SAC0807 solder alloy has a higher corrosion rate than SAC0307. The corrosion rate is also in a strong correlation with the dissolution rate of the anode and – therefore – with the ECM susceptibility as well. According to the comparison of WD tests and XPS measurements, the results are in good agreement in terms of the ECM susceptibility of SAC0807 and SAC0307 solder alloys, which means that the SAC0807 solder alloy has a lower resistance against ECM due to its high corrosion rate which is higher than that of the SAC0307 solder alloy. It can be supposed that the corrosion rate depends mainly on the microstructural and composition differences between the alloys.

4 Conclusions

According to the WD test results, the following ranking based on ECM susceptibility was found in case of the lead-free solder alloys (the lowest MTF value is the highest susceptibility): SAC 305 \geq SAC 0807 \geq SAC 405 \geq SAC 0307. The WD test results have also shown that the recently used SAC0807 solder alloy has a similarly low resistance against ECM as the lead-bearing ones. In addition, a major difference in ECM susceptibility (MTF value) was observed between the SAC0807 and SAC0307 solder alloys, despite the similar elemental composition of the dendrites. The XPS results have proven that the SAC0807 solder alloy has a significantly higher corrosion rate than the SAC0307 solder alloy, since the formed inhomogeneous SnO_x was located significantly deeper in case of SAC0807. The corrosion rate correlates to the dissolution rate of the anode, thus to the ECM susceptibility as well. Therefore, the SAC0807 solder alloy has a lower resistance against ECM (a higher ECM susceptibility) than SAC0307 due to its higher corrosion rate. So, the WD test and XPS results are in good agreement. It must be highlighted that some lead-free microalloyed low Ag content solders (e.g.: SAC0807) may pose high reliability risks in electronic devices due to the ECM failure phenomenon.

References

- 1 Directive of the European Commission for the Reduction of Hazardous Substances, (2003.) Directive 2000/0159 (COD) C5-487/2002, LEX 391, PE-CONS 3662/2/02 Rev 2, ENV581, CODEC 1273.
- 2 Muller W, Morphology changes in solder joints? experimental evidence and physical understanding, *Microelectronics Reliability*, **44**(12), (2004), 1901–1914, DOI 10.1016/j.microrel.2004.04.020.
- 3 Abtey M, Selvaduray G, Lead-free Solders in Microelectronics, *Mater Science and Engineering*, **27**(5), (2000), 95–141, DOI 10.1016/S0927-796X(00)00010-3.
- 4 McCormack M, Jin S, Kammlott G, Chen H, New Pb-free solder alloy with superior mechanical properties, *Applied Physics Letters*, **63**(1), (1993), 15–17, DOI 10.1063/1.109734.
- 5 Miller C, Anderson I, Smith J, A viable Tin–lead solder substitute: Sn?Ag?Cu, *Journal of Electronic Materials*, **23**(7), (2004), 595–601, DOI 10.1007/BF02653344.
- 6 Shohji I, Gagg C, Plumbridge W, Creep properties of Sn–8Mass%Zn–3Mass%Bi lead-free alloy, *Journal of Electronic Material*, **33**(8), (2004), 923–927, DOI 10.1007/s11664-004-0222-7.
- 7 Sharif A, Chan Y, Effect of substrate metallization on interfacial reactions and reliability of Sn–Zn–Bi solder joints, *Microelectronic Engineering*, **84**(2), (2007), 328–335, DOI 10.1016/j.mee.2006.10.087.
- 8 Takemoto T, Latanision RM, Eagar TW, Matsunawa A, Electrochemical migration tests of solder alloys in pure water, *Corrosion Science*, **39**(8), (1997), 1415–1430, DOI 10.1016/S0010-938X(97)00038-3.
- 9 Yu DQ, Jillek W, Schmitt E, Electrochemical migration of Sn–Pb and lead free solder alloys under distilled water, *Journal of Materials Science: Materials in Electronics*, **17**(3), (2006), 219–227, DOI 10.1007/s10854-006-6764-0.
- 10 Yu DQ, Jillek W, Schmitt E, Electrochemical migration of lead free solder joints, *Journal of Materials Science: Materials in Electronics*, **17**(3), (2006), 229–241, DOI 10.1007/s10854-006-6765-z.
- 11 Jung JY, Lee SB, Lee HY, Joo YC, Park YB, Effect of ionization characteristics on electrochemical migration lifetimes of Sn–3.0Ag–0.5Cu solder in NaCl and Na2SO4 solutions, *Journal of Electronic Materials*, **37**(8), (2008), 1111–1118, DOI 10.1007/s11664-008-0491-7.
- 12 He X, Azarian MH, Pecht MG, Evaluation of Electrochemical Migration on Printed Circuit Boards with Lead-Free and in-Lead Solder, *Journal of Electronic Materials*, **40**(9), (2011), 1921–1936, DOI 10.1007/s11664-011-1672-3.
- 13 Liu Y, Sun F, Zhang H, Zou P, Solderability, IMC evolution, and shear

- behavior of low-Ag Sn0.7Ag0.5Cu-BiNi/Cu solder joint*, Journal of Materials Science: Materials in Electronics, **23**(9), (2012), 1705–1710, DOI 10.1007/s10854-012-0649-1.
- 14 **Cheng F, Gao F, Zhang J, Jin W, Xiao X**, *Tensile properties and wettability of SAC0307 and SAC105 low Ag lead-free solder alloys*, Journal of Materials Science : Materials in Electronics, **46**(10), (2012), 3424–3429, DOI 10.1007/s10853-010-5231-8.
- 15 **Fenglian S, Yang L, Jiabing W**, *Improving the solderability and electromigration behavior of Low-Ag SnAgCu soldering*, In: 12th International Conference on Thermal, Mechanical and Multi-Physics Simulation and Experiments in Microelectronics and Microsystems (EuroSimE), 2011, pp. 1–5, DOI 10.1109/ESIME.2011.5765807.
- 16 **Medgyes B, Illés B, Berényi R, Harsányi G**, *In situ optical inspection of electrochemical migration during THB tests*, Journal of Materials Science-Materials in Electronics, **22**(6), (2011), 694–700, DOI 10.1007/s10854-010-0198-4.
- 17 **Zhong X, Zhang G, Qui Y, Chen Z, Zou W, Guo X**, *In situ study the dependence of electrochemical migration of tin on chloride*, Electrochemistry Communications, **27**, (2013), 63–68, DOI 10.1016/j.elecom.2012.11.010.
- 18 **Li D, Conway PP, Liu C**, *Corrosion characterization of tin-lead and lead free solders in 3.5 wt.% NaCl solution*, Corrosion Science, **50**(4), (2008), 995–1004, DOI 10.1016/j.corsci.2007.11.025.
- 19 **Jellesen MS, Minzari D, Rathinavelu U, Moller P, Ambat R**, *Corrosion failure due to flux residues in an electronic add-on device*, Engineering Failure Analysis, **17**(6), (2010), 1263–1272, DOI 10.1016/j.engfailanal.2010.02.010.
- 20 **Yang S, Wu J, Christou A**, *Initial stage of silver electrochemical migration degradation*, Microelectronics Reliability, **46**(9), (2006), 1915–1921, DOI 10.1016/j.microrel.2006.07.080.
- 21 **Harsányi G**, *Electrochemical processes resulting in migrated short failures in microcircuits*, IEEE Transactions on Components, Packaging, and Manufacturing Technology – Part A, **18**(3), (1995), 602–610, DOI 10.1109/95.465159.
- 22 **Shirley DA**, *High-Resolution X-Ray Photoemission Spectrum of the Valence Bands of Gold*, Physical Review B, **5**(12), (1972), 4709–4714, DOI 10.1103/PhysRevB.5.4709.
- 23 **Nuñez M**, *Prevention of Metal Corrosion: New Research*, Nova Science Publishers, Inc; New York, 2007, ISBN 1-59454-500-6.
- 24 **R. Subasri, T. Shinohara**, *The Applicability of SnO₂ Coatings for Corrosion Protection of Metals*, Electrochemical and Solid-State Letters, **7**(7), (2004), 17–20, DOI 10.1149/1.1737713.